energies

Article

Micro-Energy Grid Energy Utilization Optimization with Electricity and Heat Storage Devices Based on NSGA-III Algorithm

Junchao Yang [1,*] and Li Li [2]

[1] School of Account, Inner Mongolia University of Finance and Economics, Hohhot 010051, China
[2] School of Economics and Management, Beijing Information Science & Technology University, Beijing 102206, China; lilinw2001@126.com
* Correspondence: yjcim2022@yeah.net; Tel.: +86-13684787695

Abstract: With the implementation of policies to promote renewable energy generation on the supply side, a micro-energy grid, which is composed of different electricity generation categories such as wind power plants (WPPs), photovoltaic power generators (PVs), and energy storage devices, can enable the local consumption of renewable energy. Energy storage devices, which can overcome the challenges of an instantaneous balance of electricity on the supply and demand sides, play an especially key role in making full use of generated renewable energy. Considering both minimizing the operation costs and maximizing the renewable energy usage ratio is important in the micro-energy grid environment. This study built a multi-objective optimization model and used the NSGA-III algorithm to obtain a Pareto solution set. According to a case study and a comparative analysis, NSGA-III was better than NSGA-II at solving the problem, and the results showed that a higher renewable generation ratio means there is less electricity generated by traditional electricity generators like gas turbines, and there is less electricity sold into the electricity market to obtain more benefits; therefore, the cost of the system will increase. Energy storage devices can significantly improve the efficiency of renewable energy usage in micro-energy grids.

Keywords: micro-energy grid; power utilization optimization; energy and heat storage devices; NSGA-III

check for updates

Citation: Yang, J.; Li, L. Micro-Energy Grid Energy Utilization Optimization with Electricity and Heat Storage Devices Based on NSGA-III Algorithm. *Energies* **2024**, *17*, 5563. https://doi.org/10.3390/en17225563

Academic Editor: Yuji Yamada

Received: 30 August 2024
Revised: 20 October 2024
Accepted: 22 October 2024
Published: 7 November 2024

1. Introduction

With the stable economic development of China, the energy demand is also continuously increasing rapidly. Due to the characteristics of China's energy resource endowment, coal is the main primary energy source of China. It exceeds half of China's total energy demand, and it causes several serious environmental problems, such as air pollution and PM2.5 problems. Therefore, the Chinese government is focusing on the optimization of China's energy supply and demand coordination, and it has put forward the "energy supply-side reform" policy in the past five years. Increasing renewable energy generation and transforming power is considered one of the effective ways to optimize the energy supply structure under this background. The total installed capacity of China's renewable generation reached 728,960 MW as of 2019, accounting for 38.4% of China's total installed power generation, and the wind power and solar power generation reached 51.7% of the renewable power generation [1]. Renewable energy generation has exceeded the goal of China's long-term "the thirteen Five-Year Plan". China's renewable energy generation has been developed for a long time.

Due to the intermittent characteristics of a renewable energy supply, the renewable energy abandonment phenomenon is considered a big problem for renewable energy usage. In 2019, the National Energy Administration of China announced that the amount of abandoned wind power was 16.9 billion kWh, and the amount of abandoned solar power was 46 billion kWh. Determining how to make better use of renewable energy to meet the energy demand situation is a popular issue. For a power grid's safety and reliability constraints, the renewable energy ratio of the power grid connection has always been limited by 25% in China. Thus, increasing the wind power, solar power, and other renewable energy ratios in power grid connections is a big challenge for a power grid company. In order to solve this challenge, micro-energy grids have been developed, which use electricity as the central energy; combine multiple forms of energy generation; transform appliances, heat, and electricity storage devices into a system; realize multi-energy complementary system flexible integration; and use a smart dispatching system to coordinate the supply from different energy sources to meet a region's energy demand.

Storage devices play an important role in a micro-energy grid because they can handle electricity generated from different sources in different times and spaces. Due to the fact that a micro-energy grid is a new concept of energy supply, some investors have focused on an economic feasibility analysis of micro-energy grids. Recently, some scholars have studied a micro-energy grid's economic problem with energy storage devices. The potential of a micro-grid's benefits and economics with storage devices has been discussed from the perspective of reducing production costs and electricity prices [2]. He Xian took the French electricity market as an example to simulate the economics of energy system operation with air energy storage devices under different operating models and business models for achieving the maximum goal for profits [3]. Drury comparatively analyzed the air energy storage value's economic benefits with the demand response management [4], and Ding evaluated the economic value of a grid-scale energy system with storage appliances in monopoly power markets using an input–output model [5]. The above literature has established some economic analysis models under different energy system or micro-energy system environments and has pointed out that an economic analysis of energy systems or micro-energy systems should consider many important factors, such as network planning and operating costs. In addition, the energy storage technologies and sizes [6], the dispatching management [7], and the demand response need to be solved as important problems.

According to the fact that micro-energy grids always contain several types of energy generation [8], the multi-energy complementation coordination of a micro-energy grid needs to consider the participation of the demand response to promote renewable energy consumption [9] and the fact that the storage devices always act as flexible loads to participate in the regulation of the micro-grid system and the enhancement of the renewable energy generation ratio [10]. Akram studied the optimization problem of the wind, solar, and storage battery hybrid size in a micro-grid environment [11] and discussed the coordination mechanism. Shadmand studied the multi-objective optimization problem of a photovoltaic and wind hybrid system in a smart environment [12]; Sahand designed a scheduling optimization cooperation mechanism of a family-type micro-grid with a participating demand-side response; the mechanism can effectively promote renewable energy consumption [13]. Ehsan built a cooperation optimization model to deal with a micro-grid dispatching problem containing thermal power units, distributed energy, and energy storage systems [14]. Nnamdi et al. proposed an optimal economic dispatch method to solve the problem of grid-connected micro-grids consisting of photovoltaic, diesel, and wind power, and the proposed method promotes renewable energy consumption and ensures grid stability [15]. Takayama considered the uncertain characteristics of a wind power supply and designed a deterministic optimization approach to calculate the target value of wind power output; the results reduced the volatility of wind power and addressed the scheduling of wind power [16]. Hoicka proposed an optimization model to consider a family-sized micro-grid in order to partition the demand response in the electricity market and increase the residential energy consumption efficiency [17].

With the continuous development of various energy storage technologies, different energy storage devices played an increasingly important role in micro-grids [18], effectively improving renewable energy consumption, cutting peak load, filling valley load, and reducing micro-grid fluctuations [19]. A multi-energy complementary system with various energy storage devices, such as cold storage, heat storage, electric storage, and hybrid energy storage, was recently installed in a micro-energy grid environment. In this system, combined cooling, heating, and power (CCHP) was a classic application in a multi-energy complementary setup [20]. Lu gave a basic form and an optimization model to solve a multi-energy CCHP problem using a full-life bi-level iterative algorithm; the strategies for CCHP profits were discussed, and the economic feasibility of different energy storage system configurations was also analyzed [21]. Ippolito proposed a framework for a residential user micro-grid, combined with a geographic information system (GIS), to assess the spatiotemporal potential of renewable energy production fluctuations [22]. Buffat tested different control methods for micro-CCHP combined storage systems and discussed key parameters in a simulation environment for both rule-based control and optimized control situations [23]. Kneiske also tested a model for a predictive control algorithm for a PV-CHP system, and results showed that the introduction of hydrogen in natural gas would improve the cogeneration system [24]. Cinti gave a heuristic algorithm to evaluate the energy and economic balance of a micro-CHP unit and designed software to assist in micro-CHP management [25]. Marcoberardino considered the traditional demand response scheduling situation and pointed out that CCHP could be treated as a resource for response management in the electricity market [26].

Some scholars considered micro-grid management in a virtual power plant (VPP) environment, which referred to using advanced control, metering, and communication technologies to optimize the management of different types of power generation, especially for distributed and renewable energies in a micro-energy grid [27]. A Multi-Agent model was employed to study VPP optimization problems, enabling control of different energy production and storage devices, and agent-based software was used to operate a micro-grid environment [28]. The uncertainties of renewable energy production were also significant challenges in the VPP environment of a micro-grid; Yu discussed these issues and how to counter the uncertainties in a VPP environment [29]. Ju proposed a multi-objective optimization model for VPP management, where the CVAR method was used to describe uncertainties in the model, and a three-stage algorithm was applied to solve it; carbon emission allowances were also considered [30]. Ju [31] and Ghorbankhani [32] used a dynamic risk model and a bi-level stochastic model to evaluate the uncertainties of a VPP system within a demand response environment, showing that the VPP could improve efficiency and increase demand-side resource participation in the power market. Pourghaderi et al. also proposed that technical virtual power plants (TVPPs) play an important role in activating commercial consumers in demand response programs [33]. However, when numerous distributed energy sources and residents participate in the electricity market, traditional power grid architectures cannot efficiently consume renewable energy or manage energy dispatching. A more effective approach involved adding storage devices to enhance the flexibility of renewable energy production and consumption [34], allowing demand-side resources to participate more flexibly and efficiently in electricity market transactions. Han et al. developed a two-tier optimization model for Load-Serving Entities (LSEs) in the Day-Ahead (DA) market that considered grid-level energy storage (ES) and virtual power plants (VPPs), demonstrating that VPPs, when used with ES, have a complementary function of peaking and valley-filling, which aids in coordinating the integration of renewable energy sources [35]. Tan et al. proposed a VPP system structure containing ES devices with optimal scheduling, showing that this configuration could improve wind power efficiency usage and manage peak and valley rates [36].

The micro-energy grid was a new concept and form of smart grid construction in China, and the micro-energy grid with the energy storage devices brought a significant reform of China's energy supply and energy consumption structures. From the above studies, it is obvious that the storage devices played an important role in the micro-energy grid environment. The micro-energy grid environment was always considered as a single region of energy supply and consumption systems like a micro-grid, and the above studies focused on optimizing system operating costs. However, the micro-energy grid could also be considered as a participant of a power supplier or a power demander in the electricity market. The key issues included determining how to optimize the micro-energy grid's energy utilization in the electricity market to achieve lower operating costs and higher renewable energy ratios, and why it was essential for a micro-energy grid to incorporate energy storage devices. Although many scholars studied optimization problems related to micro-energy grid utilization, most focused on either economic or dispatch energy supply schedules to meet demand, with only a few addressing the multi-objective optimization problem (MOP). Therefore, we considered the micro-grid MOP, aiming to satisfy both economic efficiency and maximum renewable energy utilization with various energy storage devices, including electric and heat storage, in the micro-grid, and we employed an improved NSGA-III algorithm to solve this problem.

The rest of the paper is organized as follows: Section 2 presents the mathematical model for electric and heat storage devices. Section 3 describes a multi-optimization model, NSGA-III, for a micro-energy grid with storage devices, considering both operating costs and renewable energy electricity generation. Section 4 introduces the NSGA-III algorithm. Section 5 provides a case study and discussion, and finally, the conclusion is given in Section 6.

2. Mathematics Models of Storage Devices in a Micro-Energy Grid

In a micro-energy grid, different storage devices flexibly balance energy supply and consumption while promoting the consumption of renewable energies. The most common types of storage are electric storage and heat storage, and the mathematical models are given as follows:

(1) Electric storage

Electricity, as a secondary energy source, always plays an important role in different energy transformations within a micro-energy grid environment, especially for renewable energies like wind and solar. Electric storage devices store excess energy supply and provide power when energy is insufficient in a micro-energy grid. Currently, China primarily installs lithium iron phosphate batteries as the main electric storage devices in micro-energy grids due to their high energy density, large storage capacity, and extended scheduling period. The battery's energy storage capacity depends on charge power and efficiency, with its mathematical model expressed in Equation (1).

$$E_{EES,t} = \begin{cases} E_{ESS,t-1} + \theta \eta_{ele}^{+} g_{ESS,t}^{+} - (1-\theta) \eta_{ele}^{-} g_{ESS,t}^{-} & t > 1 \\ E_{ESS,0} & t = 1 \end{cases} \quad (1)$$

In this model, $E_{EES,t}$ represents the energy storage devices' capacity at time t; $g_{ESS,t}^{+}$ and $g_{ESS,t}^{-}$ denote the charging and discharging power of the energy storage devices at time t; η_{ele}^{+} and η_{ele}^{-} refer to the efficiency of the energy storage devices. The variable θ is a binary indicator where the value is 1 when the energy storage is charging and 0 otherwise.

The constraints of the energy storage devices are as follows:

(1) The energy storage level should not exceed the device's maximum capacity.

$$E_{EES,\min} \leq E_{EES,t} \leq E_{EES,\max} \quad (2)$$

(2) The charging or discharging power at time t should not exceed the device's design power limit.

$$\begin{cases} g_{EES,\min}^{+} \leq g_{EES,t}^{+} \leq g_{EES,\max}^{+} \\ g_{EES,\min}^{-} \leq g_{EES,t}^{-} \leq g_{EES,\max}^{-} \end{cases} \quad (3)$$

(2) Heat storage

Cogeneration, or combined heat and power (CHP), enabled the cascade utilization of energy and was commonly used during the winter season in northern China. Renewable energy sources such as wind or solar often generate electricity during periods of low energy demand; however, heat demand is typically high at these times. In such situations, CHP could not be fully utilized, leading to significant renewable energy curtailment. Heat storage technology allowed for interaction with renewable energy, effectively enhancing the flexibility and economy of a micro-energy grid and thereby increasing the share of renewable energy consumption. When both heat energy storage and electric energy storage operated simultaneously, they contributed to smoothing the energy storage system's output curve, extended the system's service life, and facilitated coordinated management of both electric and heat storage devices.

The characteristics of heat energy storage devices could be calculated by the relationship between storage capacity, output power, input power, and heat efficiency. The mathematical model is as follows:

$$H_{TES,t} = \begin{cases} H_{TES,t-1} + \delta\eta_{heat}^{+}q_{heat,t}^{+} - (1-\delta)\eta_{heat}^{-}q_{heat,t}^{-} & t > 1 \\ H_{TES,0} & t = 1 \end{cases} \tag{4}$$

Here, $H_{TES,t}$ is the power in heat storage devices at time t; $q_{heat,t}^{+}$ and $q_{heat,t}^{-}$ refer to charge and discharge power of the heat storage devices at time t; η_{heat}^{+} and η_{heat}^{-} refer to the efficiency of the heat storage devices, δ is a binary variable where the value is 1 when the heat storage device is charging and 0 otherwise.

Similarly, the constraints of heat storage devices are as follows:

(1) The heat storage should not exceed the limited capacity of devices.

$$H_{TES,\min} \le H_{TES,t} \le H_{TES,\max} \tag{5}$$

(2) The charging or discharging power of heat storage devices at time t should not exceed the limit of the design power.

$$\begin{cases} q_{heat,\min}^{+} \le q_{heat,t}^{+} \le q_{heat,max}^{+} \\ q_{heat,\min}^{-} \le q_{heat,t}^{-} \le q_{heat,max}^{-} \end{cases} \tag{6}$$

3. Optimization Models of a Micro-Grid with Storage Devices

3.1. Multi-Objective Functions

A typical micro-grid system in North China is generally regarded as a multi-energy management system composed of wind energy, solar energy, and natural gas turbines. The system can be divided into a power subsystem and a thermal subsystem. The power subsystem includes small wind power generation clusters, photovoltaic power generation clusters, traditional gas turbines, and lithium iron phosphate batteries, which serve as electricity storage devices. The thermal subsystem includes solar thermal, electric boilers, and heat storage tanks. All devices and subsystems are uniformly controlled and communicated by a central controller, and the system interacts with a power distribution network tie line. The system structure is shown in Figure 1.

The energy management of the micro-energy grid system focuses on two main objective functions. One is reasonably arranging the output of each device to minimize the operating costs, including decisions on whether to connect with the external power grid to buy or sell the electricity according to the real-time market prices. The other is to coordinate and optimize the dispatch of renewable energy generators, electric boilers, gas turbines, electricity storage devices, and heat storage devices to meet both the energy and heat demands and promote the maximization of the system's renewable generation ratio. The first objective function of the minimum operating cost mathematics model is

$$\min obj_1 = \sum_{t=1}^{T} (C_{CGT,t} + C_{ele,t} + C_{EB,t} + C_{EES,t} + C_{TES,t} - R_{ele,t}) \tag{7}$$

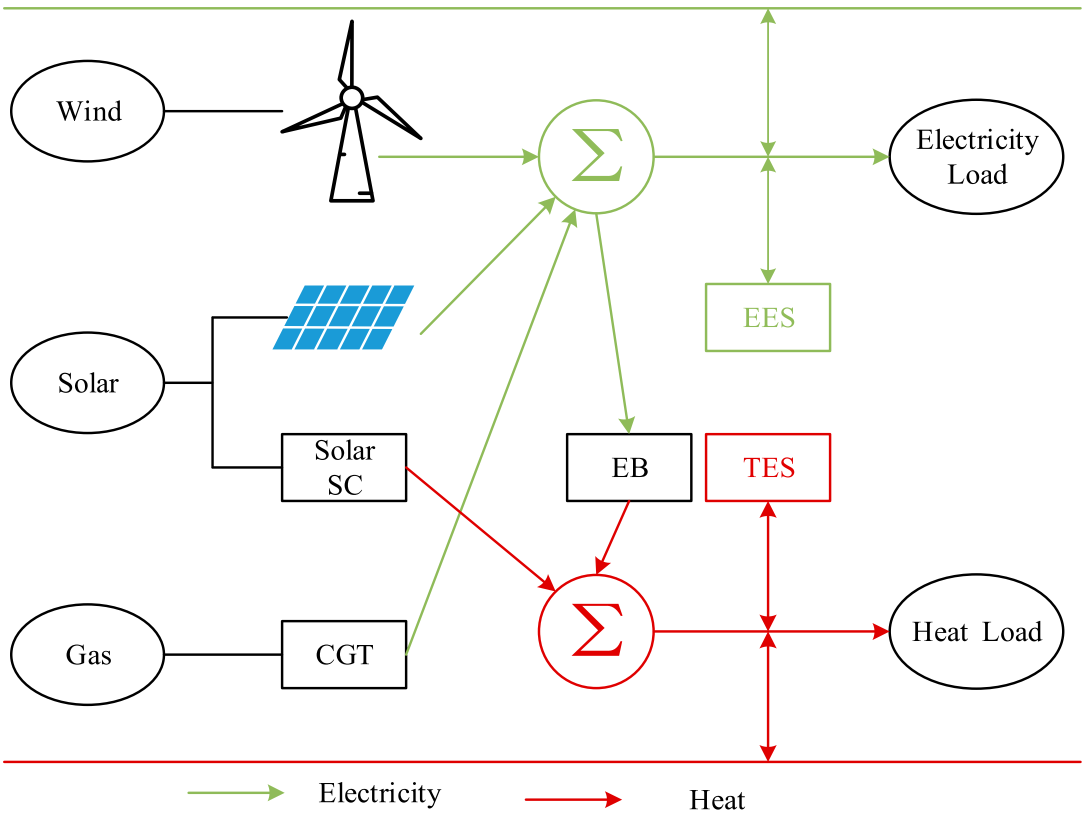

Figure 1. A typical micro-energy grid environment.

Here, $C_{ele,t}$ is the cost of purchasing electricity from the external power grid; it equals the product of the real-time electricity price p_{ele} and the total purchased electricity q_{ele}. $C_{EB,t}$ represents the operating cost of the electric boiler, $C_{EES,t}$ and $C_{TES,t}$ indicate the running costs of electricity and heat storage, and $R_{ele,t}$ is the electricity sales of the external power grid. $C_{CGT,t}$ is the running cost of the gas turbine at time t, which can be calculated with the product of the gas price $price_{Gas,t}$ and gas consumption $Gas_{CGT,t}$ at time t. When the gas turbine starts or stops running, its cost also includes the respective starting or stopping costs.

$$C_{CGT,t} = price_{Gas,t} * Gas_{CGT,t} \tag{8}$$

The gas consumption $Gas_{CGT,t}$ can be expressed as a quadratic function with the output power of gas turbine at time t.

$$Gas_{CGT,t} = ap^2_{CGT,t} + bp_{CGT,t} + c \tag{9}$$

The other objective function is the maximization of the renewable energy generation ratio in the micro-energy grid's energy supply, and the mathematical model is

$$\max obj_2 = \frac{1}{E_{Total}} \sum_{t=1}^{T} (E_{wpp,t} + E_{pv,t}) \tag{10}$$

Here, E_{Total} is total energy supply of time T, and $E_{wpp,t}$ and $E_{pv,t}$ are the energy supply of wind energy generation and solar energy generation.

The above equation is equivalent to

$$\min obj_2 = 1 - \frac{1}{E_{Total}} \sum_{t=1}^{T} (E_{wpp,t} + E_{pv,t}) \tag{11}$$

3.2. Constraint Functions

The system must satisfy both the energy balance and operation constraints.

(1) Energy balance constraints. Energy supply should equal the energy demand at time t, with the constraint given by

$$\min obj_2 = 1 - \frac{1}{E_{Total}} \sum_{t=1}^{T} (E_{wpp,t} + E_{pv,t}) \tag{12}$$

Here, $g_{w,t}$, $g_{pv,t}$, and $g_{CGT,t}$ represent the total power supply of wind energy generation, solar energy generation, and CGT generation, respectively. $g^{-}_{EES,t}$ is the discharging power of electricity storage devices, $g^{+}_{EES,t}$ is charging power, $g_{EB,t}$ is the power of the electric boiler, and L_t is the total load of the micro-energy grid at time t.

(2) Heat balance constraints. Similarly, heat supply should also be equal to heat demand at time t, with the constraint given by

$$Q_{SC,t} + Q_{EB,t} + Q^{+}_{heat,t} + Q^{-}_{heat,t} = Q_t \tag{13}$$

Here, $Q_{SC,t}$ is the heat supply from the SC device, $Q_{EB,t}$ is the heat supply of the electric boiler at time t, $Q^{+}_{heat,t}$ and $Q^{-}_{heat,t}$ are the discharging and charging power from the heat storage devices, respectively, and Q_t is the total heat demand at time t.

3.3. Calculation of Constraint Parameters

The calculation of each power output from related electricity devices is shown as follows:

(1) Electricity output $g_{w,t}$ calculation of the wind turbine. The electricity output of the wind turbine is determined by wind speed, and the output presents a piecewise-defined function by different wind speeds, it is also limited by wind turbine technical parameter C_w limits.

$$g_{w,t} = \begin{cases} 0 \quad 0 \le v_t < v_{in}, v_t \ge v_{out} \\ 0.5 C_w \rho A_{wt} v_t^3 \; v_{in} \le v_t \le v_p \\ g_p \quad v_p \le v_t \le v_{out} \end{cases} \tag{14}$$

When the wind speed is lower than the cut-in speed of the wind turbine v_{in} or higher than the cut-out speed v_{out}, the wind turbine will stop generating electricity. If the wind speed is between v_{in} and the rated wind speed v_p, the output is calculated as the product of 0.5, C_w, the air density ρ, and the projection of the swept area of wind turbine blades on the vertical plane of wind speed $A_{wt} v_t^3$ and wind speed v_t. Otherwise, the output is the rated power g_p of the wind turbine.

(2) Electricity output $g_{pv,t}$ calculation of photovoltaic generation. Photovoltaic electricity generation is based on the photovoltaic effect of the semiconductor interface, which directly converts the absorbed solar energy to electricity, and the output $g_{pv,t}$ can be calculated as

$$g_{pv,t} = [1 - \gamma(T_{air} + \frac{T_n - 20}{800}\theta_t - T_{ref})]\eta_{pv}\theta_t S_{pv} N_{pv} \tag{15}$$

Here, γ is the photoelectric conversion efficiency of the photovoltaic panel, T_{air} is the air temperature of the atmosphere, T_n is the normal operating temperature, and T_{ref} and η_{pv} are the reference temperature and reference efficiency for photovoltaic generation, respectively; θ_t is the light radiation intensity at time t, S_{pv} is the area of each photovoltaic panel, and N_{pv} is the number of photovoltaic panels.

Photovoltaic power generation is also characterized by randomness, intermittency, and fluctuation. Its output intensity is related to the intensity of light radiation θ, which consistently follows a Beta distribution function with parameters α and β. The equation is

$$f(\theta) = \begin{cases} \frac{\theta^{\alpha-1}(1-\theta)^{\beta-1}}{\int_0^1 \theta^{\alpha-1}(1-\theta)^{\beta-1} d\theta} & 0 \le \theta \le 1, \beta \ge 0 \\ 0 & otherwise \end{cases} \tag{16}$$

The distribution function of the intensity of light radiation is

$$P(\theta) = \int_{\theta_{\min}}^{\theta_{\max}} f(\theta) d\theta \tag{17}$$

The parameters α and β can be estimated from history data of the intensity of light radiation, if the mean value is μ and the variance is σ^2, then α and β can be calculated by

$$\begin{cases} \beta = (1-\mu)(\frac{\mu(1+\mu)}{\sigma^2} - 1) \\ \alpha = \frac{\mu\beta}{1-\mu} \end{cases} \tag{18}$$

(1) Electricity output $g_{CGT,t}$ calculation of gas turbine. The gas turbine generates electricity by burning natural gas to drive the generator rotor to rotate at a high speed, and the waste heat is recovered through a waste heat boiler. As a traditional power generation device, a CGT plays a significant role in a micro-energy grid, with its output mainly determined by the gap between renewable generation and electricity demand. The relationship of the output power $g_{CGT,t}$, power generation efficiency η_c, and gas turbine exhaust is

$$g_{CGT,t} = \eta_c L_{NG} V_{NG} \tag{19}$$

L_{NG} is the calorific value of natural gas, generally taken as 9.7 KW h/m^3, and V_{NG} represents the amount of natural gas consumed by the gas turbine during operation. η_c denotes the power generation efficiency of the gas turbine.

(2) Heat output $Q_{SC,t}$ calculation of solar heat devices.
The heat output $Q_{SC,t}$ can be calculated by the following equations:

$$Q_{SC,t} = F_R WL[S_t - \frac{U_{lo}}{C}(T_t^{in} - T_{air})] \tag{20}$$

Here, W and L are the length and width of the solar collector tube, T_t^{in} is the inlet temperature of the light and heat collector at time t, T_{air} is the air temperature at time t, U_{lo} denotes total loss coefficient, C is the concentration ratio, F_R is the operational transmission ratio of the photothermal system, and F_R is the total effective flux absorbed by the surface at time t.

(3) Heat output $Q_{EB,t}$ calculation of the electric boiler.

Electric boilers are simple to install, flexible to control, and easy to maintain and replace, making them widely used in micro-energy grids. The heat output $Q_{EB,t}$ of the electric boiler at time t is

$$Q_{EB,t} = 3.6\eta_{EB} g_{EB,t} \tag{21}$$

Here, η_{EB} represents the heat conversion efficiency of the electric boiler, and $g_{EB,t}$ denotes the electric power consumed by the electric boiler at time t.

4. NSGA-III Algorithm

The optimization model is a multi-objective optimization problem (MOP), for which several solution algorithms are available. Over the past two decades, with intelligent algorithm studies, the evolutionary multi-objective optimization (EMO) algorithms have generally considered to be effective algorithms for solving MOPs because EMO can find the Pareto-optimal boundary easily and flexibly. The Nondominated Sorting Genetic Algorithm (NSGA) is the most common EMO algorithm for solving MOPs and is based on a genetic algorithm (GA). NSGA applies a nondominated sorting approach, which increases the likelihood that high-quality individuals are passed on to the next generation, and it uses a shared fitness strategy to evenly distribute solutions along the quasi-Pareto front. This approach helps maintain the diversity of the population, limits the overproduction of super-individuals, and prevents the premature convergence of the algorithm.

NSGA-III is a newly developed NSGA algorithm based on NSGA-II, reducing the complexity of NSGA and achieving a well-converged solution with ease. Since NSGA-III is similar to NSGA-II, and the only difference is that NSGA-III has added the adaptive updating of a set of well-spread reference points, we first introduce NSGA-II. NSGA-II has an elite strategy to ensure that some high-performing individuals are retained throughout the evolution process. Additionally, NSGA-II adopts the crowding distance comparison operator to overcome the defect of NSGA needing to manually specify shared parameters, so that the individuals in the quasi-Pareto concentration can be evenly expanded to the whole Pareto domain, ensuring the diversity of the population [37]. The flow of the NSGA-II algorithm is illustrated in Figure 2.

NSGA-II uses traditional crossover and mutation operators, as in the GA algorithm, with its advantage reflected in three core operators that select the high-performing parents to generate offspring.

(1) Fast Nondominated Sorting
Fast Nondominated Sorting ranks the population according to each individual's dominance level, guiding the search toward the Pareto front. For each p in the population, P, it counts the number of individuals dominating p in the population and denotes the number as p_n, and then it sorts the individuals into several levels. The main steps of Fast Nondominated Sorting are as follows:
   (1) Set all individuals with $p_n = 0$ into a set F.
   (2) For each individual F_i in F, group individuals dominated by F_i into a set S. For each individual S_i in S, let the number of individuals dominating $p_n = p_n - 1$. Add all individuals with $p_n = 0$ into set F_1 as the second level.
   (3) Repeat the above two steps until the entire population is classified.

(2) Crowding-distance calculation

For each individual i within the same level F_i, the crowding-distance degree d_i is calculated based on the distances between its two adjacent individuals' objective function values F_{i-1} and F_{i+1} by

$$d_i = \sum_{m=1}^{m} \frac{f_m^{i+1} - f_m^{i-1}}{f_m^{\max} - f_m^{\min}} \tag{22}$$

Here, f_m is the m-th objective function, and $f_m^{\max}$ and $f_m^{\min}$ represent the maximum and the minimum values of the m-th objective function, respectively. For individuals located at the edge of each level F_i, meaning those with the maximum and the minimum values, the crowding distance is defined as $d_1 = d_N = \infty$.

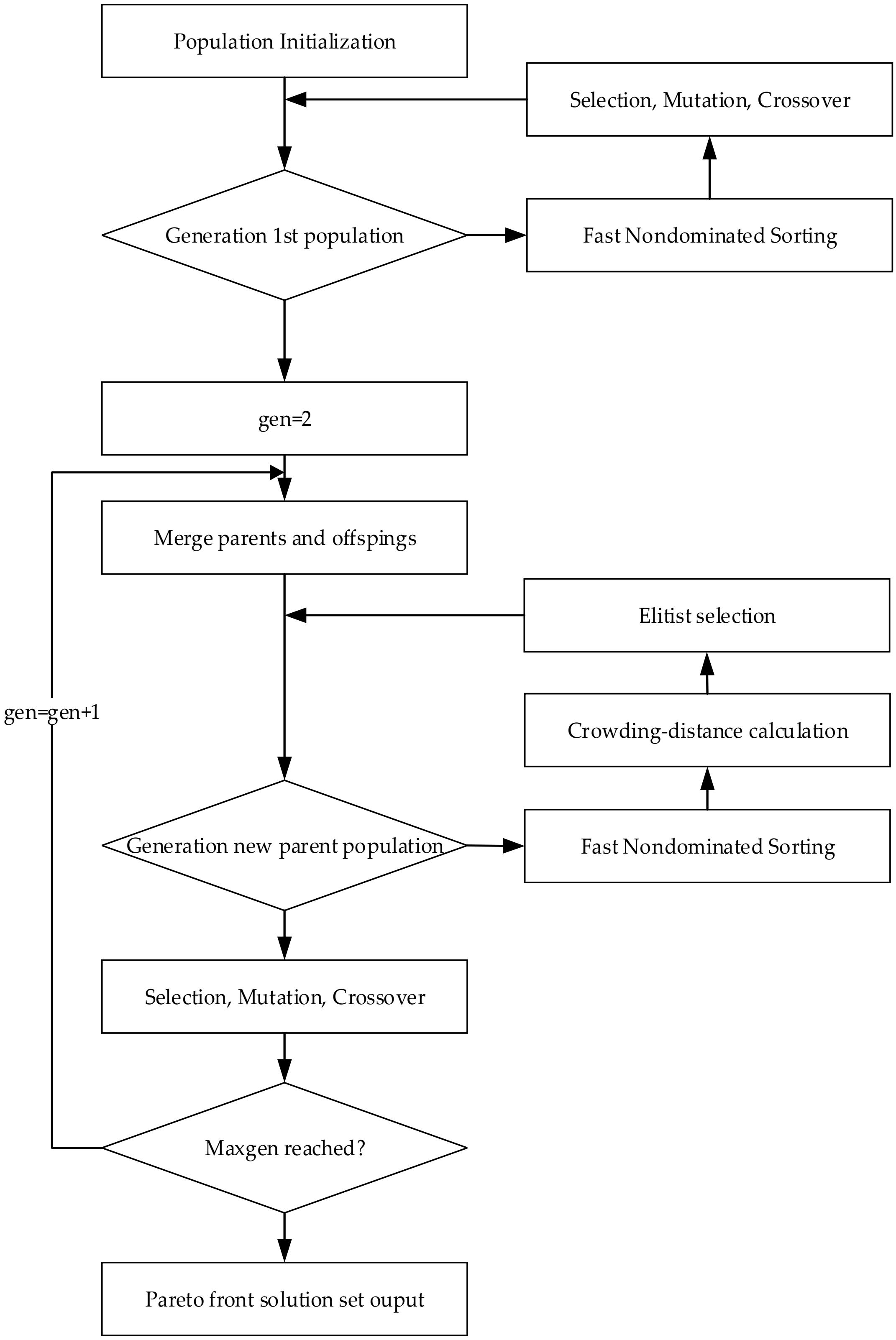

Figure 2. NSGA-II algorithm.

Using Fast Nondominated Sorting and the crowding-distance calculation, each individual i has two attributes: the nondominated sort level F_i and crowding distance d_i. Based on the two attributes, we define that individual i is better than individual j if either $F_i < F_j$ or $F_i = F_j$ and $d_i > d_j$.

(3) Elitist Selection

NSGAII employs an elitist selection strategy to preserve high-quality individuals from the parent population in the offspring, preventing population degeneration and avoiding the loss of the Pareto solution that has been obtained. Initially, a random parent population P_0 of size N is created, followed by usual selection, crossover, and mutation operators to create an offspring population Q_0 of size N. A $2N$ size population set R_0 is formed by $P_0 \cup U_0$. The individuals in R_0 are subjected to nondominated sorting, and each individual's nondominated sort level F_i and crowding distance di are calculated. The top N individuals based on these metrics are selected as the next generation of offspring. P_1 repeats the process until the maximum number of iterations is reached, and the final individuals in F_1 can be considered as the Pareto solutions.

In NSGA-III, the crowding distance operator is improved with the following improvements: (1) classification of the population into nondominated levels, (2) determination of distributed reference points on a Hyper-Plane, (3) adaptive determination of the number and location of the reference points based on the number of targets and population size, and (4) the introduction of an association operation. In the above processes, the NSGA-III algorithm not only considers the nondominated level of each individual, but also considers the individual's reference point association, that is, the distance between the individual and the reference point and the crowding of the reference point, which can better balance the diversity and convergence of the population, helping to avoid over-selection or neglect of certain targets, and further details can be found in reference [38].

5. Case Study and Result Discussion

5.1. Data Collection

We select a typical multi-energy integrated system in the Etuoke Economic Development Zone of Inner Mongolia, established in April 2001. This zone, located in Qipanjing Town, Etuoke Banner, Ordos City, Inner Mongolia, spans a total area of 25 square kilometers primarily developed for industry, with a population of 82,000. It is a typical energy and heavy chemical base in the western part of Inner Mongolia Autonomous Region, with coal and electricity production as its core. Winter is chosen for this study, as the system requires much more heat energy during this season than in others. The system includes several small wind power plants (WPPs) with 3 × 2.5 MW installed capacity, a 3 × 1 MW small photovoltaic (PV) power generation unit, a conventional gas turbine (CGT) with 5 × 1 MW installed capacity, an electric boiler (EB) with the maximum 4.2 MW capacity, solar thermal 2 × 1 MW clusters, an electric energy storage (EES) device, and a thermal energy storage (TES) device. The parameters of the storage devices and the systems are shown in Tables 1 and 2.

Table 1. Energy storage and heat energy storage parameters.

Equipment	Maximum Capacity (MW)	Efficiency (η)	Cost (CNY/kWh)
EES	4	0.9	0.8
TES	2	0.9	0.6

The real electricity price and gas price in this area are divided into three periods: peak, flat, and valley, as shown in Table 3.

The WPP and PV electricity generation can be calculated using the parameters in Table 2 and Equations (13)–(17). Wind speed data are based on the average wind speed for the same season of the last year, as shown in Figure 3. This paper uses the scene simulation method to generate 50 groups of simulation scenes [39], with the scene of the highest occurrence probability selected as the generated output data for the case study. The generation output results for a typical day of WPP and PV generation are shown in Figure 4.

Table 2. Parameters of the systems.

Equipment	Parameters	Value
CGT	coefficient $a,\ b,\ c$ of $Gas_{CGT,t}$	2.66×10^{-4}, 0.3137, 0.01327
	eta_c	0.75
WPP	C_w	0.45
	ρ	$1.225\ \mathrm{kg/m^3}$
	A_{wt}	$4.298 \times 10^4\ \mathrm{m^2}$
	v_{in}	4 m/s
	v_p	14 m/s
	v_{out}	25 m/s
PV	α	0.39
	β	8.45
EB	eta_{EB}	0.85

Table 3. Electricity and gas prices.

Type	Peak Period	Flat Period	Valley Period
Electricity period	8:00–12:00, 17:00–22:00	12:00–17:00, 22:00–24:00	0:00–8:00
Electricity price (CNY/kWh)	0.90	3.00	0.45
Gas period	21:00–9:00, 12:00–15:00, 18:00–19:00	19:00–21:00	9:00–12:00, 15:00–18:00
Gas price (CNY)	3.75	3.00	2.50

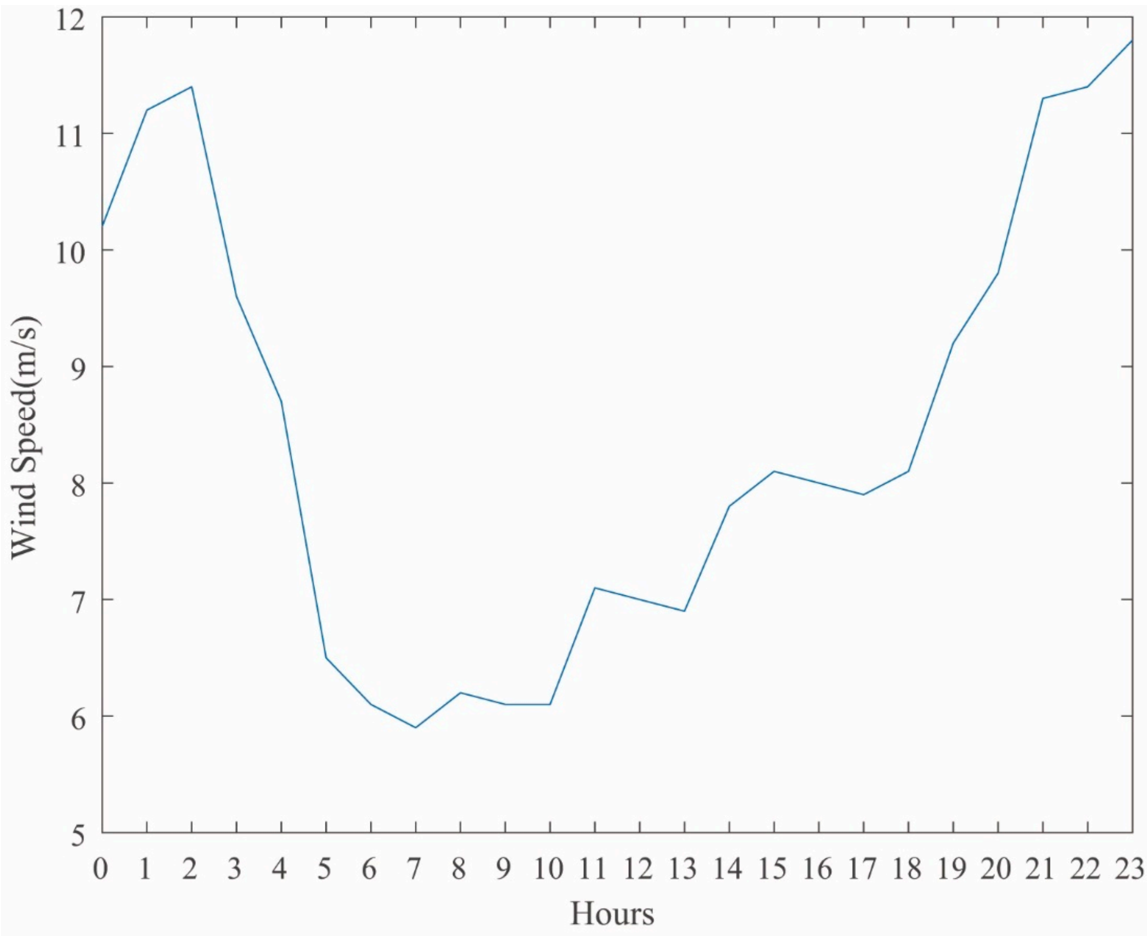

Figure 3. Wind speed.

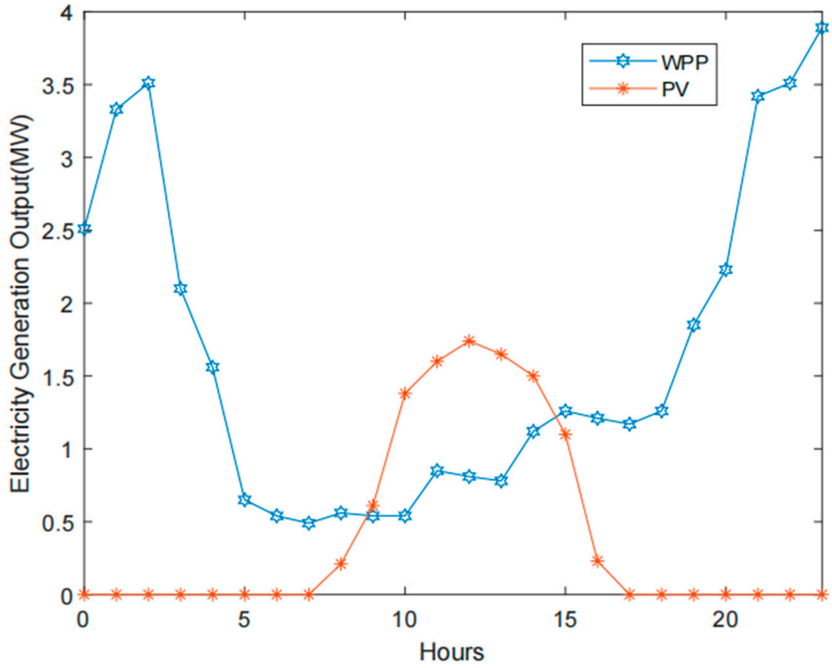

Figure 4. Electricity generation output of WPP and PV devices.

The typical daily electricity and heat demand data of the system are shown in Figure 5. These data are based on the data collection of the system in each hour, using the average values of 24 h in December of last winter. The maximum electricity and heat demands are 4.05 MW and 3.62 MW, occurring at 18:00 and 1:00, respectively.

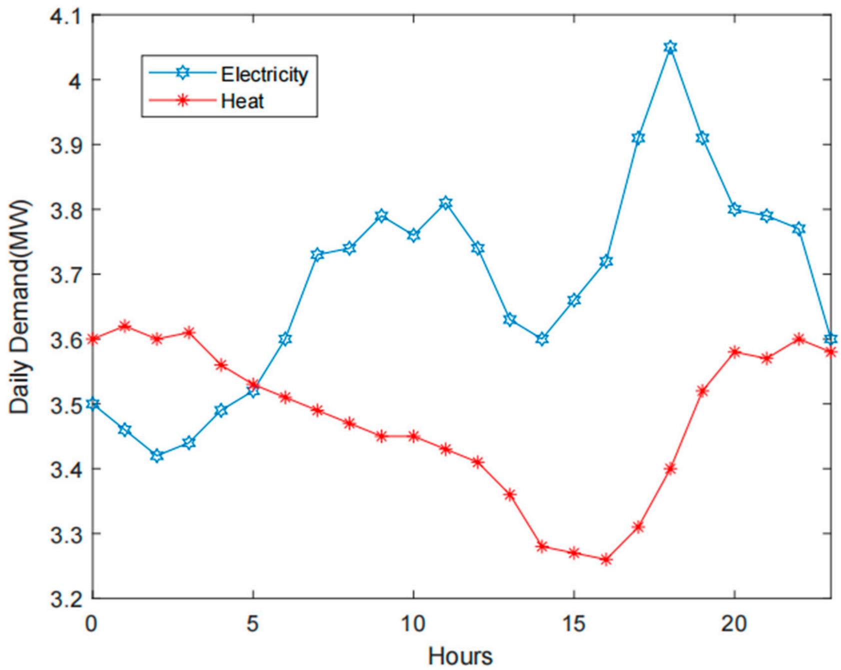

Figure 5. Typical daily electricity and heat demand data.

5.2. Result Comparison for NSGA-III, NSGA-II, and MOPSO

We use NSGA-III to solve the multi-energy integrated system's MOP; the population of NSGA-III is 100, the crossover rate is 0.7, the mutation rate is 0.4, and the maximum iteration number is 500. All the parameters are the default values of the source code supplied by Deb's personal website. We modify the code based on our model to solve this MOP. For comparison, we also employ the NSGA-II, which shares the same parameters as NSGA-III mentioned above, and we also employ the Common Multiple objective with the particle swarm optimization (MOPSO) algorithm. The source code of NSGA-II and MOPSO is also supplied by Deb's website. The results can be compared in Table 4.

Table 4. Result comparison for NSGA-III, NSGA-II, and MOPSO.

Solution	NSGA-III	NSGA-II	MOPSO
Min Cost	9815.5	10,147	10,166
Max renewable ratio	39.32%	39.42%	37.6%
Nondominated solution No.	9	16	The best one

From Table 4, we observe that NSGA-III and NSGA-II yield 9 and 16 nondominated solutions, respectively, while MOPSO provides only the global best swarm solution. More solutions always mean that decision-makers have more decision reference points. The minimum cost and maximum renewable ratio appear in different solutions, and the solutions for the minimum cost and maximum renewable ratio obtained with NSGA-III and NSGA-II outperform those from MOPSO. Among the three algorithms, NSGA-III's solutions demonstrate the best performance.

5.3. Result Comparison Between NSGA-III and NSGA-II

The final NSGA-III Pareto solutions in set F1 are shown in Figure 6a, and the number of F1 is 9. The two edge points' values of F1 are (9815.5, 68.49%) and (10,083.2, 60.68%), indicating that the minimum operating cost's range is [9815.5, 10,083.2], while the minimum CGT electricity supply ratio's range is [60.68%, 68.49%]. This is equivalent to the maximum renewable electricity supply ratio range of 31.51% to 39.32% in Figure 6a. Comparably, the results of the NSGA-II Pareto solutions in set F1 are shown in Figure 6b. The number of F1 is 16. The two edge points' values of F1 are (10,147, 61.57%) and (10,328.7, 60.58%), meaning the minimum operating cost's range is [10,328.7, 10,147], and the minimum CGT electricity supply ratio range is [60.58%, 61.57%]. This is equivalent to the maximum renewable electricity supply ratio being within [38.43%, 39.42%]. Although the number of Pareto solutions in NSGA-III is lower than in NSGA-II, the performance of the results is superior. The solutions are more center-distributed, and the values of both obj-1 and obj-2 have improved. And the reason for the minimum cost is more electricity generated by the CGT being sold to the power grid during peak electricity pricing, yielding higher system benefits. Respectively, if the system aims for a higher renewable generation ratio, it needs to limit the electricity generation by the CGT, resulting in lower electricity sales to the power grid and a higher operating cost.

The electricity and heat supply at the two extreme points of NSGA-III in F_1 are shown in Figure 7. Figure 7a presents the minimum operating cost solution, where the system includes more CGT electricity generation and EES charging participation. This configuration enables more electricity to be sold in the electricity market, typically after 9:00 when prices are higher, allowing the system to gain more benefit from the electricity market and thus reducing costs. The other side illustrates the highest renewable energy ratio situation. In this case, the system purchases electricity from the electricity market at 4:00, 6:00, 7:00, and 9:00, while EES discharges are more frequently used to lower the CGT electricity generation ratio.

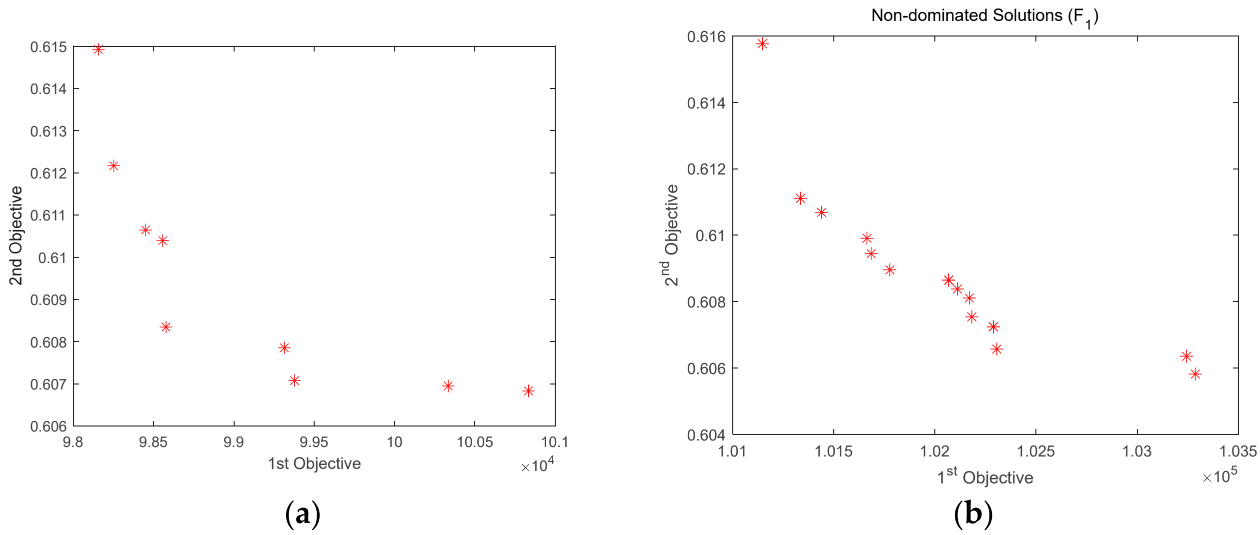

Figure 6. Pareto solutions of the multi-energy integrated system's MOP. (**a**) NSGA-III Pareto solutions; (**b**) NSGA-II Pareto solutions.

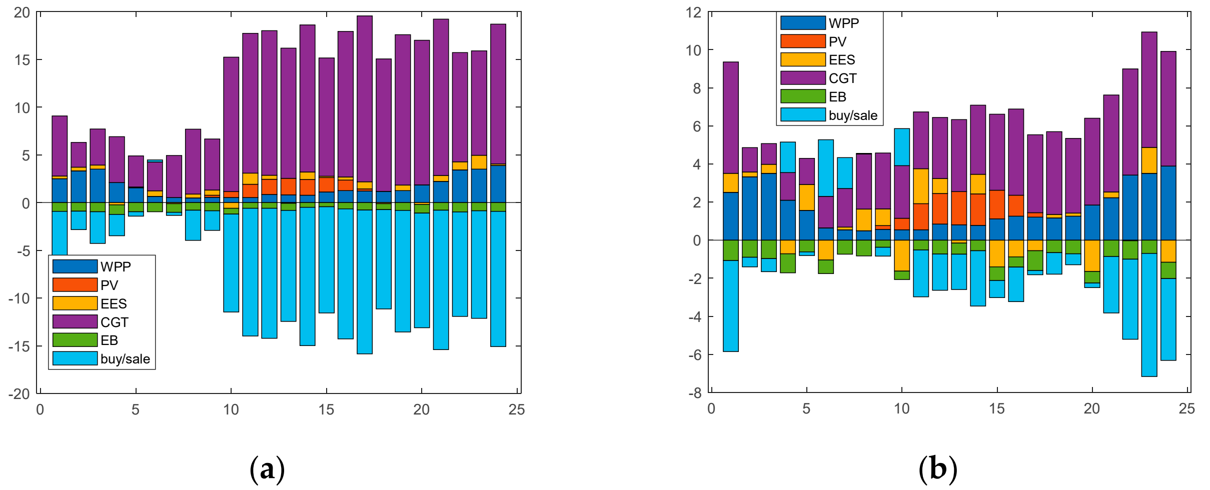

Figure 7. Two edge points' electricity supply of the NSGA-III Pareto solutions with EES and TES. (**a**) Minimize operating cost; (**b**) maximize renewable energy generation ratio.

Figure 8 presents the results of NSGA-III F1 solutions for the heat supply at the two extreme points. Figure 9a shows the maximum heating capacity of the electricity boiler, which will result in increased gas usage and some abandonment of SC heat from PV generation. On the other hand, in Figure 9b, the maximum renewable energy generation ratio's results indicate that more TES systems participate in the system's heat supply than in the minimum operation cost scenario. This approach reduces the heat from EB, and it indirectly lowers electricity consumption, which can reduce the CGT electricity generation and enhance the renewable energy generation ratio.

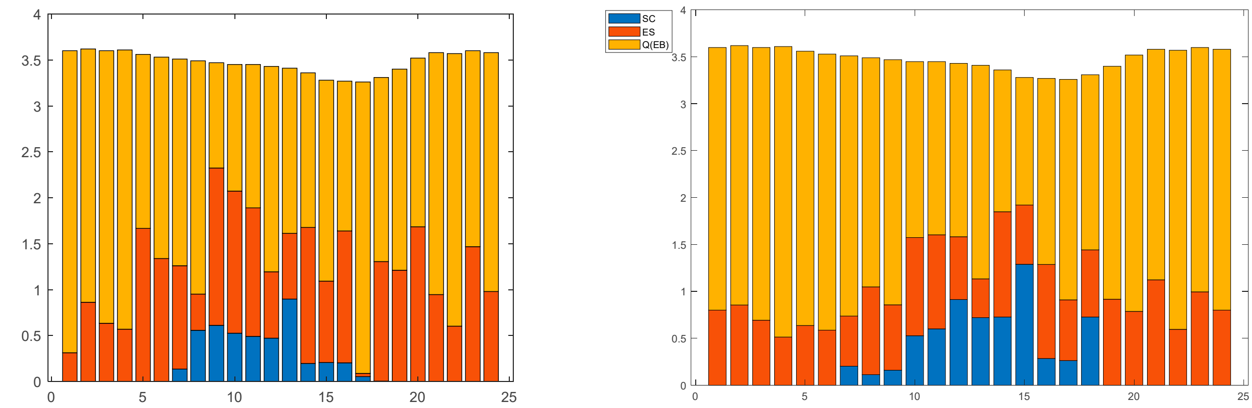

(**a**) (**b**)

Figure 8. Two edge points' heat supply of the Pareto solutions with EES and TES. (**a**) Minimize operating cost; (**b**) maximize renewable energy generation ratio.

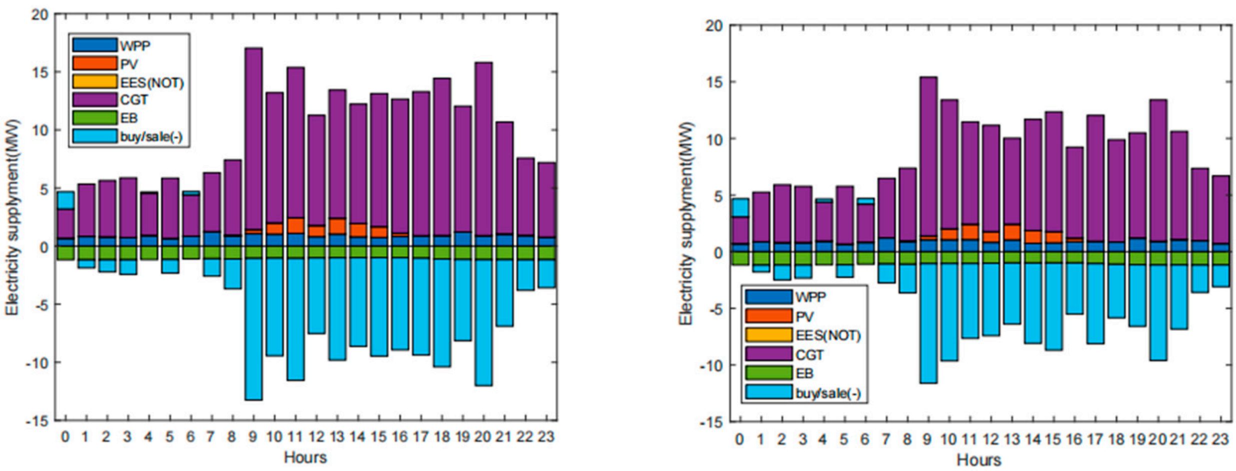

(**a**) (**b**)

Figure 9. Two edge points' electricity supply of the Pareto solutions without EES and TES. (**a**) Minimize operating cost; (**b**) maximize renewable energy generation ratio.

5.4. Storage Device Function Discussion

In order to analyze the effect of the storage devices' usage in the system, we also run the NSGA-III algorithm without EES and TES included. In this situation, the renewable electricity ratio is limited to 25% at any time t to ensure system safety and reliability. The Pareto solutions without EES and TES show that the system cost ranges from 13,712.47 to 19,672.45, and the CGT electricity generation ratio is between 86.21% and 86.42%. The two edge points in F_1 are also shown in Figures 9 and 10. Similarly, the minimum operating cost is due to more electricity being sold in the electricity market during high-price periods, while a lower CGT electricity generation ratio indicates less electricity is sold in the electricity market. The main difference in the electricity supply with and without EES devices is in the output of the WPP and PV electricity generation in the system. As shown in Figure 7, both WPP and PV devices operate at full capacity when adjusted by EES and TES. However, without EES and TES adjustments, WPP and PV devices must curtail some wind and solar resources to meet the system's reliability constraints.

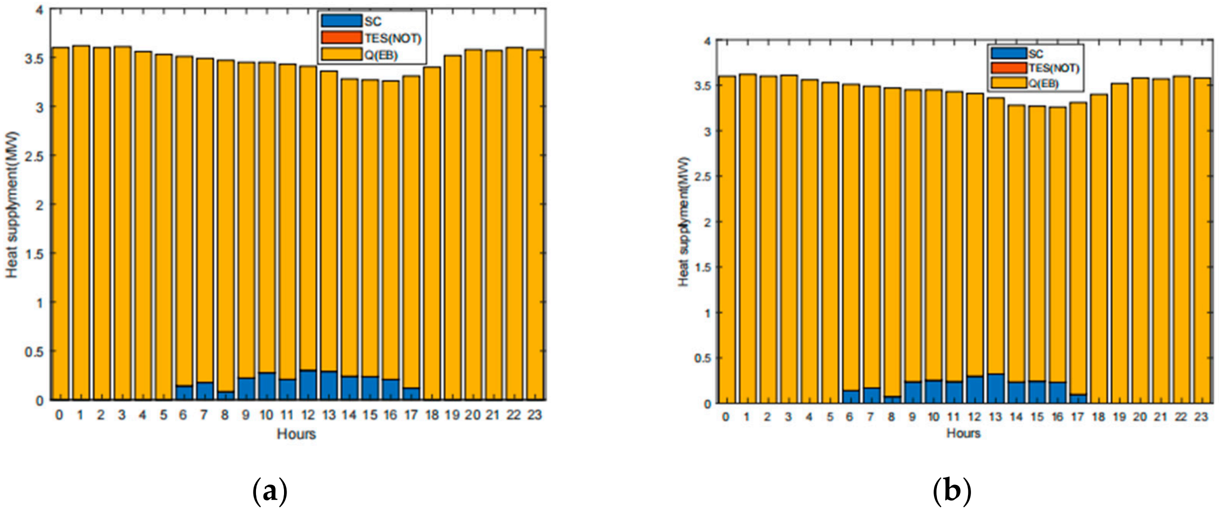

Figure 10. Two edge points' heat supply of the Pareto solutions without EES and TES. (**a**) Minimize operating cost; (**b**) maximize renewable energy generation ratio.

The heat supply illustrated in Figure 10 indicates that more heat is generated by the EB without TES, which leads to a higher electricity demand for the EB. This, in turn, indirectly increases the electricity supply from the CGT, thereby raising the overall cost of the whole system.

The heat supply results in both situations are nearly identical because the heat demand is entirely met by SC and EB devices without TES. The heat output from SC is limited by solar energy availability, making the heat from EB the primary source in the system. Given that the heat demand is fixed, there is no additional capacity for heat adjustment from either SC or EB without TES.

6. Conclusions

This study developed a multi-objective optimization model for a micro-energy grid environment incorporating WPP, PV, CGT, EB, EES, and TES devices. The NSGA-III algorithm was employed to solve for the Pareto solutions of the model. Based on the case study, the following conclusions have been drawn:

(1) This paper is a typical study applicable to micro-energy grids in industrial parks. The multi-objective optimization model of a micro-energy grid environment considered WPP, PV, CGT, EB, EES, and TES devices in the paper, so if the study object is a more complex grid, other types of equipment need to be considered, and the optimization model needs to be adjusted appropriately. In addition, the WPP and PV devices in this optimization model have significant requirements related to environmental factors (such as sunshine intensity, wind speed, temperature, humidity, and altitude), making this study particularly applicable to regions with abundant renewable resources and favorable climatic conditions. The inclusion of EB and TES is more critical in colder regions, whereas their usage is less necessary in areas with moderate year-round temperatures. Thus, this study is especially relevant for regions with substantial seasonal temperature variations, like northern China. By utilizing data from Inner Mongolia, a province known for its rich renewable energy resources and high winter heat demand, this research provides valuable insights for the investment and development of micro-energy grids in industrial parks. The optimization model and algorithm can also be extended to other regions with abundant renewable resources and significant heat energy needs.

(2) The energy supply of a micro-energy grid comprises diverse sources, including wind, solar, and traditional fossil fuels. Compared to a single-fossil-fuel supply environment, a micro-energy grid with a diversified energy supply creates a favorable setting for

promoting renewable energy usage. The storage devices EES and TES work in tandem with various energy generation sources to meet regional electricity and heat demands while maximizing the utilization of renewable energy. Comparative analysis shows that a micro-grid equipped with EES and TES can significantly reduce the operating cost associated with energy supply and enhance the maximum electricity output power from WPP and PV devices. Conversely, without energy storage devices, if the micro-energy grid's energy supply system does not include the energy storage devices, the electricity generated from WPP and PV devices would be constrained by safety and reliability requirements.

(3) The multi-objective model takes into account both operating costs and the ratio of renewable energy usage, meaning that the Pareto solutions aim to minimize operating costs while maximizing renewable energy utilization simultaneously. Analyzing two endpoints of the Pareto solutions reveals that if the system focuses on minimizing operating costs, it will generate more electricity from the CGT and sell it in the electricity market during peak price periods to maximize profits. Conversely, if the system prioritizes maximizing the renewable energy usage ratio, the electricity generated from the CGT will be limited, resulting in lower income from electricity sales in the market. The Pareto solutions provide a range of more decision-making options for stakeholders, allowing them to respond. Decision-makers can make different decisions in response to the changes in the external environment. For example, considering the low carbon emissions associated with renewable energy generation, governments may encourage its adoption through subsidies, green certificates, and quota systems. In such cases, it may be more effective for decision-makers to accept a certain degree of economic sacrifice to enhance the proportion of renewable energy in their energy mix.

In addition, as the cost of energy storage continues to decline in the future, the integration of storage devices within a micro-energy grid environment is expected to rise, thereby enhancing the capacity for renewable energy generation. A well-reasoned and optimized configuration of storage devices in a micro-grid can not only improve the overall benefits of energy supply but also effectively promote the electricity consumption generated by renewable sources such as WPP and PV devices.

Given these findings, the study offers significant implications for governments, grids, and micro-grid investors.

Based on the results of this optimization model, the government could adopt policies such as subsidies, green certificates, and carbon quotas to incentivize investors to increase the installed capacity of wind power plants and photovoltaic power. This would lead investors to prioritize renewable energy usage more in the trade-off between cost reduction and increased renewable energy usage, thus promoting renewable energy development and assisting in the realization of the "Carbon peaking and carbon neutrality goals".

For the power grid, the model demonstrates that by increasing the price difference between peak and off-peak hours, the grid can incentivize micro-grid investors to store electricity during off-peak periods for sale during peak hours, allowing investors to profit. This approach is essential for grid peaking and frequency regulation.

For micro-grid investors, the Pareto solutions presented in this paper can provide a reference for micro-grid operation decisions. In addition, micro-grid investors can balance cost reduction and renewable energy use by adjusting to external environment changes to achieve optimal decisions.

Author Contributions: Conceptualization, J.Y.; Investigation, L.L.; Methodology, J.Y.; Software, J.Y.; Supervision, L.L.; Validation, J.Y.; Visualization, L.L.; Writing—Original Draft, J.Y.; Writing—Review and Editing, J.Y. and L.L. All authors have read and agreed to the published version of the manuscript.

Funding: This research received no external funding.

Data Availability Statement: The original contributions presented in the study are included in the article; further inquiries can be directed to the corresponding authors.

Acknowledgments: We thank Yongfeng Qiao who helped with the English improvements.

Conflicts of Interest: The authors declare no conflicts of interest.

References

1. British Petroleum. *Statistical Review of World Energy 2019*; Technical Report; British Petroleum: London, UK, 2019.
2. Das, T.; Krishnan, V.; McCalley, J.D. Assessing the benefits and economics of bulk energy storage technologies in the power grid. *Appl. Energy* **2015**, *139*, 104–118. [CrossRef]
3. He, X.; Lecomte, R.; Nekrassov, A.; Delarue, E.; Mercier, E. Compressed air energy storage multi-stream value assessment on the french energy market. In Proceedings of the 2011 IEEE PowerTech, Trondheim, Norway, 19–23 June 2011. [CrossRef]
4. Drury, E.; Denholm, P.; Sioshansi, R. The value of compressed air energy storage in energy and reserve markets. *Energy* **2011**, *36*, 4959–4973. [CrossRef]
5. Ding, J.; Xu, Y.; Chen, H.; Sun, W.; Hu, S.; Sun, S. Value and economic estimation model for grid-scale energy storage in monopoly power markets. *Appl. Energy* **2019**, *240*, 986–1002. [CrossRef]
6. Bahramirad, S.; Reder, W.; Khodaei, A. Reliability-Constrained Optimal Sizing of Energy Storage System in a Microgrid. *IEEE Trans. Smart Grid* **2012**, *3*, 2056–2062. [CrossRef]
7. Vahidinasab, V. Optimal distributed energy resources planning in a competitive electricity market: Multiobjective optimization and probabilistic design. *Renew. Energy* **2014**, *66*, 354–363. [CrossRef]
8. Zhang, Y.; Iu, H.H.C.; Fernando, T.; Yao, F.; Emami, K. Cooperative Dispatch of BESS and Wind Power Generation Considering Carbon Emission Limitation in Australia. *IEEE Trans. Ind. Inform.* **2015**, *11*, 1313–1323. [CrossRef]
9. Jiang, Y.; Xu, J.; Sun, Y.; Wei, C.; Wang, J.; Ke, D.; Li, X.; Yang, J.; Peng, X.; Tang, B. Day-ahead stochastic economic dispatch of wind integrated power system considering demand response of residential hybrid energy system. *Appl. Energy* **2017**, *190*, 1126–1137. [CrossRef]
10. Howlader, H.O.R.; Matayoshi, H.; Senjyu, T. Distributed generation integrated with thermal unit commitment considering demand response for energy storage optimization of smart grid. *Renew. Energy* **2016**, *99*, 107–117. [CrossRef]
11. Akram, U.; Khalid, M.; Shafiq, S. Optimal Sizing of a Wind/Solar/Battery Hybrid Grid-connected Microgrid System. *IET Renew. Power Gener.* **2017**, *12*, 72–80. [CrossRef]
12. Shadmand, M.B.; Balog, R.S. Multi-Objective Optimization and Design of Photovoltaic-Wind Hybrid System for Community Smart DC Microgrid. *IEEE Trans. Smart Grid* **2014**, *5*, 2635–2643. [CrossRef]
13. Behboodi, S.; Chassin, D.P.; Djilali, N.; Crawford, C. Interconnection-wide hour-ahead scheduling in the presence of intermittent renewables and demand response: A surplus maximizing approach. *Appl. Energy* **2017**, *189*, 336–351. [CrossRef]
14. Reihani, E.; Motalleb, M.; Thornton, M.; Ghorbani, R. A novel approach using flexible scheduling and aggregation to optimize demand response in the developing interactive grid market architecture. *Appl. Energy* **2016**, *183*, 445–455. [CrossRef]
15. Nwulu, N.I.; Xia, X. Optimal dispatch for a microgrid incorporating renewables and demand response. *Renew. Energy* **2017**, *101*, 16–28. [CrossRef]
16. Takayama, S.; Ishigame, A. Study on the ramp fluctuation suppression control of wind power generation output using optimization method. *Electr. Eng. Jpn.* **2018**, *205*, 8–15. [CrossRef]
17. Hoicka, C.E.; Parker, P. Assessing the adoption of the house as a system approach to residential energy efficiency programs. *Energy Effic.* **2018**, *11*, 295–313. [CrossRef]
18. Salehpour, M.J.; Tafreshi, S.M. The effect of price responsive loads uncertainty on the risk-constrained optimal operation of a smart micro-grid. *Int. J. Electr. Power Energy Syst.* **2019**, *106*, 546–560. [CrossRef]
19. Mansour-lakouraj, M.; Shahabi, M. Comprehensive analysis of risk-based energy management for dependent micro-grid under normal and emergency operations. *Energy* **2019**, *171*, 928–943. [CrossRef]
20. Rostamzadeh, H.; Ebadollahi, M.; Ghaebi, H.; Shokri, A. Comparative study of two novel micro-CCHP systems based on organic Rankine cycle and Kalina cycle. *Energy Convers. Manag.* **2019**, *183*, 210–229. [CrossRef]
21. Lu, S.; Li, Y.; Xia, H. Study on the configuration and operation optimization of CCHP coupling multiple energy system. *Energy Convers. Manag.* **2018**, *177*, 773–791. [CrossRef]
22. Ippolito, F.; Venturini, M. Micro Combined Heat and Power System Transient Operation in a Residential User Microgrid. *J. Energy Resour. Technol.* **2018**, *141*, 042006. [CrossRef]
23. Buffat, R.; Raubal, M. Spatio-temporal potential of a biogenic micro CHP swarm in Switzerland. *Renew. Sustain. Energy Rev.* **2019**, *103*, 443–454. [CrossRef]
24. Kneiske, T.M.; Niedermeyer, F.; Boelling, C. Testing a model predictive control algorithm for a PV-CHP hybrid system on a laboratory test-bench. *Appl. Energy* **2019**, *242*, 121–137. [CrossRef]
25. Cinti, G.; Bidini, G.; Hemmes, K. Comparison of the solid oxide fuel cell system for micro CHP using natural gas with a system using a mixture of natural gas and hydrogen. *Appl. Energy* **2019**, *238*, 69–77. [CrossRef]
26. Di Marcoberardino, G.; Chiarabaglio, L.; Manzolini, G.; Campanari, S. A Techno-economic comparison of micro-cogeneration systems based on polymer electrolyte membrane fuel cell for residential applications. *Appl. Energy* **2019**, *239*, 692–705. [CrossRef]
27. Zhang, G.; Jiang, C.; Wang, X. Comprehensive review on structure and operation of virtual power plant in electrical system. *IET Gener. Transm. Distrib.* **2018**, *13*, 145–156. [CrossRef]

28. Gao, Y.; Zhou, X.; Ren, J.; Wang, X.; Li, D. Double Layer Dynamic Game Bidding Mechanism Based on Multi-Agent Technology for Virtual Power Plant and Internal Distributed Energy Resource. *Energies* **2018**, *11*, 3072. [CrossRef]
29. Yu, S.; Fang, F.; Liu, Y.; Liu, J. Uncertainties of virtual power plant: Problems and countermeasures. *Appl. Energy* **2019**, *239*, 454–470. [CrossRef]
30. Ju, L.; Tan, Q.; Lu, Y.; Tan, Z.; Zhang, Y.; Tan, Q. A CVaR-robust-based multi-objective optimization model and three-stage solution algorithm for a virtual power plant considering uncertainties and carbon emission allowances. *Int. J. Electr. Power Energy Syst.* **2019**, *107*, 628–643. [CrossRef]
31. Ju, L.; Li, P.; Tan, Z.; Wang, W. A dynamic risk aversion model for virtual energy plant considering uncertainties and demand response. *Int. J. Energy Res.* **2019**, *43*, 1272–1293. [CrossRef]
32. Ghorbankhani, E.; Badri, A. A bi-level stochastic framework for VPP decision making in a joint market considering a novel demand response scheme. *Int. Trans. Electr. Energy Syst.* **2018**, *28*, e2473. [CrossRef]
33. Pourghaderi, N.; Fotuhi-Firuzabad, M.; Moeini-Aghtaie, M.; Kabirifar, M. Commercial Demand Response Programs in Bidding of a Technical Virtual Power Plant. *IEEE Trans. Ind. Inform.* **2018**, *14*, 5100–5111. [CrossRef]
34. Han, H.; Cui, H.; Gao, S.; Shi, Q.; Fan, A.; Wu, C. A Remedial Strategic Scheduling Model for Load Serving Entities Considering the Interaction between Grid-Level Energy Storage and Virtual Power Plants. *Energies* **2018**, *11*, 2420. [CrossRef]
35. Tan, Z.F.; Li, H.H.; Ju, L.W.; Tan, Q.K. Joint Scheduling Optimization of Virtual Power Plants and Equitable Profit Distribution Using Shapely Value Theory. *Math. Probl. Eng.* **2018**, *2018*, 3810492. [CrossRef]
36. Newbery, D. Shifting demand and supply over time and space to manage intermittent generation: The economics of electrical storage. *Energy Policy* **2018**, *113*, 711–720. [CrossRef]
37. Deb, K.; Pratap, A.; Agarwal, S.; Meyarivan, T.A.M.T. A fast and elitist multiobjective genetic algorithm: NSGA-II. *IEEE Trans. Evol. Comput.* **2002**, *6*, 182–197. [CrossRef]
38. Deb, K.; Jain, H. An Evolutionary Many-Objective Optimization Algorithm Using Reference-Point-Based Nondominated Sorting Approach, Part I: Solving Problems with Box Constraints. *IEEE Trans. Evol. Comput.* **2014**, *18*, 577–601. [CrossRef]
39. Zakariazadeh, A.; Homaee, O.; Jadid, S.; Siano, P. A new approach for real time voltage control using demand response in an automated distribution system. *Appl. Energy* **2014**, *117*, 157–166. [CrossRef]